HAZARDOUS WASTE & HAZARDOUS MATERIALS
Volume 12, Number 4, 1995
Mary Ann Liebert, Inc.

Mn-Catalyzed Oxidation of Naphthalenediol

GENE WHELAN and RONALD C. SIMS

Division of Environmental Engineering
Civil and Environmental Engineering Department
Utah State University
Logan, UT 84322-4110

ABSTRACT

This study investigates the effects that manganese(IV) dioxide particles have on 2,3-naphthalenediol at varying pH levels (i.e., initial pH of 4.58, 5.85, and 8.75) and under different organic concentration conditions ($4x10^{-3}$, $4x10^{-4}$, and $4x10^{-5}$ M), and assesses the importance of Mn oxides on abiotic catalysis of the multiple-ringed aromatic compound. Proton concentration affected the rates of reductive dissolution; as the pH values increased, the rate of reductive dissolution decreased, as predicted by theory. Also, as the concentration of naphthalenediol increased, the rate of reductive dissolution increased, although not proportionally; thus indicating that a majority of the active sites had been occupied. In addition, the results tend to confirm that electron transfer/organic release from the oxide surface is the rate-limiting step. This study demonstrates that in an oxic environment and in the presence of 2,3-naphthalenediol, MnO_2 particles undergo reductive dissolution; in the process, naphthalenediol is oxidized. An oxidation by-product of reductive dissolution is an insoluble polymerized organic. The organic by-product was deep-brown in appearance, very similar to that of "humified" material. Using infrared spectroscopy, energy-dispersive x-ray analysis, and a microelemental analysis, the "humified" products appeared to be comprised mainly of constituents originating from naphthalenediol.

INTRODUCTION

Manganese(III/IV) is widely distributed within the environment. Because of its redox potential, Mn is frequently involved in redox reactions that take place at the mineral/water interface; as such, overall rates of organic oxidation depend on the organic/surface-oxide interaction (i.e., sorption, diffusion, electron transfer, etc.) [1-3]. Research has demonstrated that Mn oxides can oxidize single-ringed aromatic compounds containing hydroxl, methoxy, carboxylic, diol, and/or dione functional groups and the two-ringed-aromatic naphthol ($C_{10}H_7OH$) [4-7].

Research of other investigators has also demonstrated the potential oxidation of larger multiple-ringed aromatics, such as benzo(a)pyrene and pyrene [8,9]. Radiolabelled studies have shown that significant amounts of these polynuclear aromatic compounds have become tightly bound to sterile soil residue, so much so, the researchers were unable to remove the radiolabelled carbons though various extraction procedures. These researchers also found significant quantities of radiolabel humic and fulvic acid fractions, suggesting a humification process.

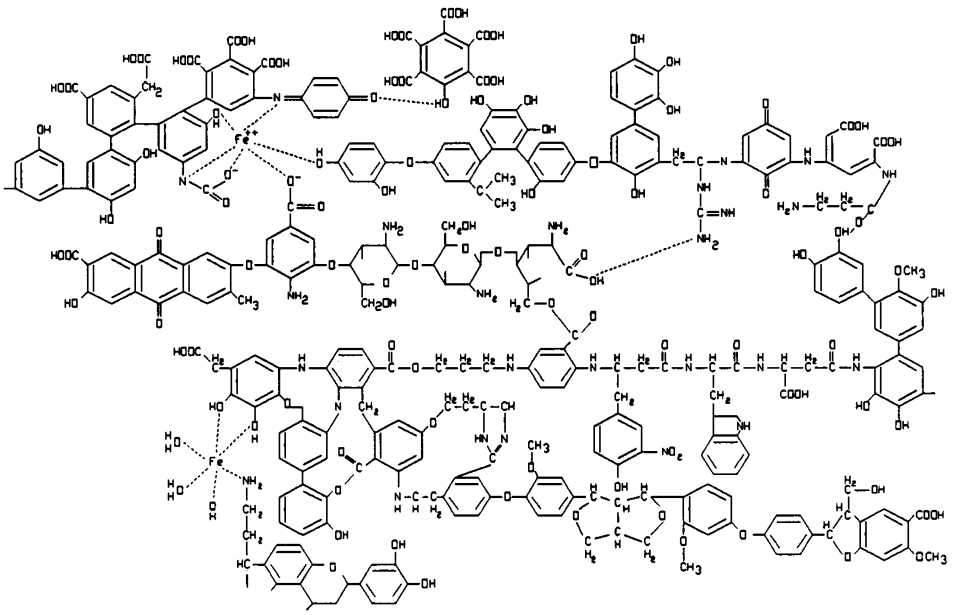

FIGURE 1. Illustrative Example of Humus [14].

Similar results were documented in biotic studies where chemical binding involving humic material was reported [10-13]. Bollag and Myers [10] concluded that polymerization of xenobiotics in the humification process is possible because many of the degradation products of organics (e.g., pesticides) result in the formation of reactive intermediates with structures and/or functional groups similar to those found in natural humic material (see Figure 1).

More information is required regarding the reaction between multiple-ringed aromatics and metal oxides. The purpose of this study was to address one aromatic chemical and to investigate its interaction with Mn oxide particles with respect to changes in pH and organic substrate concentration. In addition, this study was to investigate the potential for the formation of insoluble polymerized organic products resulting from the reductive-dissolution process.

METHODS AND MATERIALS

Unless otherwise stated all solutions were prepared from reagent grade chemicals and deionized distilled water (DDW) and filtered with a 0.2-μm-pore-diameter, nylon membrane filter (Nylaflo, Baxter Scientific Products) prior to use. All glassware was soaked in 2 N HNO_3 and 0.05 M $NH_2OH{\cdot}HCl$, and thoroughly rinsed with DDW prior to use. Reagent-grade chemicals were used in these experiments, including 2,3-naphthalenediol (Aldrich 98%). All standards, controls, and blanks were prepared in the same matrix as the samples following the same procedures outlined by Whelan and Sims [15].

The experimental design, following the procedures of Whelan and Sims [15] and Whelan [16], focused on monitoring Mn and the parent organic substrate using Inductively Coupled Plasma and High Performance Liquid Chromatography (HPLC), respectively. The Mn particles were prepared using a procedure based on Murray [17] and Godtfredsen [18]. The specific surface area associated with the MnO_2 particles were determined using a Brunauer-Emmett-Teller (BET) surface-area analyzer (Quantachrome Monosorb). The point of zero net charge (PZNC) was determined using KCl as an indifferent electrolyte and was monitored with ICP and ion chromatography. Potassium-cation concentrations were measured using a Perkin-Elmer ICP/6000 with a detection limit to 0.2 mg/L. Chloride-anion concentrations were measured fol-

lowing the U.S. Environmental Protection Agency's Method 300 [19] for the determination of inorganic anions in water. A Dionex Ion Chromatograph (IC) was used to monitor Cl^- ions; it contained the following Dionex components: automated sampler, eluent-degas and basic-chromatography modules, conductivity detector, and gradient pump. The output was monitored with an HP-3396A integrator. The columns used were an IONPAC AS4A-SC 4x250 mm (10-32) analytical column (P/N 043175) and an IONPAC AG4A-SC guard column 4x50 mm (P/N 043175). The buffer was a carbonate (1.8 mM Na_2CO_3)-bicarbonate (1.7 mM $NaHCO_3$) solution, and the regenerant was a $7.32x10^{-3}$ M H_2SO_4 solution. The flow rate was 2 mL/min, and the injection volume was 5 mL.

A series of triplicate 50-mL KIMAX centrifuge tubes with Teflon-lined septa (Thomas Scientific, 2390-H72) and screw caps were prepared under oxic conditions for each sample, blank, and control; no attempt was made to establish an anoxic environment. Two sets of samples were prepared; they assessed changes in the dissolved Mn^{2+} concentrations due to variations in pH and 2,3-naphthalenediol concentrations. Both sets of conditions contained approximately $3x10^{-4}$ M MnO_2 and $1.0x10^{-3}$ M $NaClO_4$ to help fix the ionic strength.

Three different 2,3-naphthalenediol concentrations were prepared: $4x10^{-5}$, $4x10^{-4}$, and $4x10^{-3}$ M. Each sample tube was buffered with $1.00x10^{-3}$ M acetate-buffer ($6.95x10^{-4}$ M sodium acetate and $3.48x10^{-4}$ M acetic acid) solution (initial pH of buffer measured at 4.58).

Three different pH levels were also prepared at initial pH values of 4.58, 5.85, and 8.75. Each sample tube contained a 2,3-naphthalenediol concentration of $4x10^{-4}$ M. Two different buffers were used to help fix the pH at three different levels. One third of the sample tubes were buffered with $1.00x10^{-3}$ M acetate-buffer ($6.95x10^{-4}$ M sodium acetate and $3.48x10^{-4}$ M acetic acid) solution (initial pH of buffer measured at 4.58), one third were buffered with $1.00x10^{-3}$ M acetate-buffer ($9.5x10^{-4}$ M sodium acetate and $4.8x10^{-5}$ M acetic acid) solution (initial pH of buffer measured at 5.85), and one third were buffered with $1.0x10^{-3}$ M bicarbonate-buffer ($4.8x10^{-5}$ M Na_2CO_3 and $9.5x10^{-4}$ M $NaHCO_3$) solution (initial pH of buffer measured at 8.75).

RESULTS

The ion adsorption method was used to help assess the PZNC and to determine the cation and anion exchange capacities (CEC and AEC, respectively) of the Mn oxide particles employed in this study. The results of the ion adsorption analysis are summarized in Figure 2; the mean value of triplicates with 95% confidence intervals are included for each point. The CEC ranged from 655 $mmol_c/kg$ at pH of 2.09 to 1653 $mmol_c/kg$ at pH of 4.54. The AEC was relatively small, ranging from 140 $mmol_c/kg$ at a pH of 2.09 to zero at pH values >3. Only pH levels <5 were analyzed because the PZNC is <5.

Figures 3 and 4 and Figures 5 and 6 present the effects that variations in pH and concentration, respectively, have on the reductive dissolution of Mn(III/IV) to dissolved Mn(II) and oxidation of 2,3-naphthalenediol. Figures 3 and 5 present the temporal variation in the dissolved Mn concentration by initial pH and concentration, respectively, expressed as a fraction of the total Mn added to the reaction vessel. Correspondingly, to indicate the degree of oxidation of the parent organics by the Mn particles, Figures 4 and 6 present the fraction of the organic oxidized (molar ratio of organic oxidized to organic control). The results in Figures 4 and 6 assume that separate organic controls are indicative of the initial concentration in the reaction vessel. Because separate reaction vessels are employed for the organic analyses (i.e., separate samples, controls, and blanks without subsampling), this assumption may be violated when variability between the controls are too great [15,16].

Three analyses were performed to determine the origin of the experimental precipitate observed in the study: infrared (IR) spectroscopy; microelemental determination for carbon, oxygen, and hydrogen; and scanning electron microscopy using an energy-dispersive x-ray analysis (EDXRA). The IR results are presented in Figure 7 and plot percent transmission versus frequency (in wave numbers). The EDXRA results are presented in Figure 8 and identify the major elements in the residue.

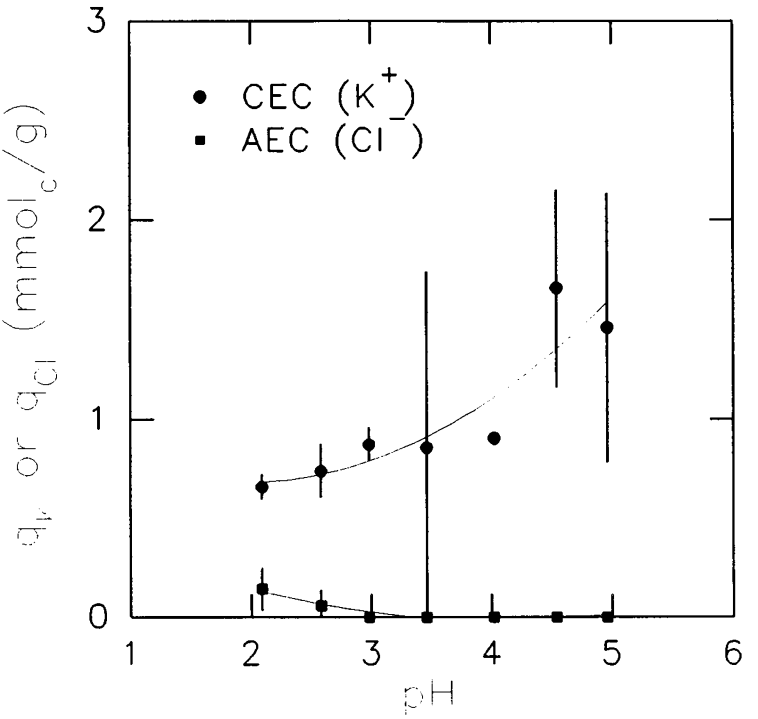

FIGURE 2. Variations is Surface Charge with pH for Manganese Oxide Particles with 95% Confidence Intervals.

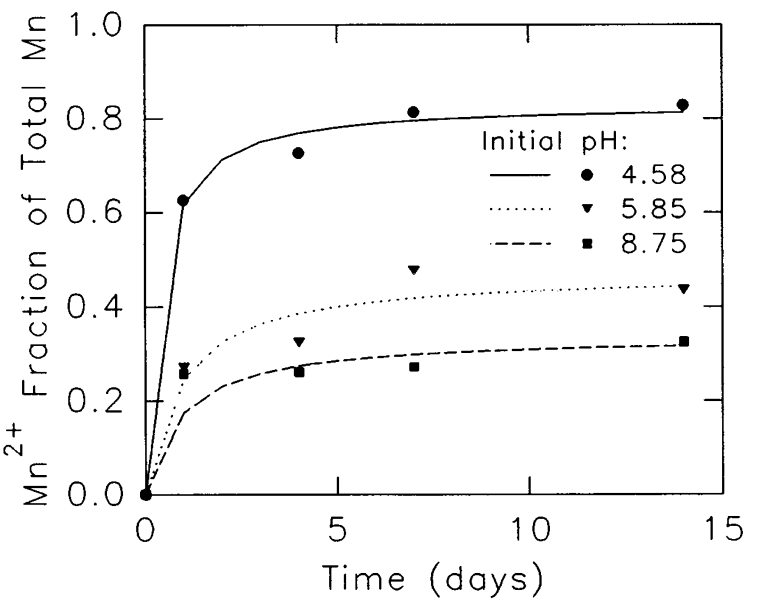

FIGURE 3. Time-Varying Fraction of Total Manganese as Dissolved Mn^{2+} for an Initial Concentration of $4x10^{-4}$ M as a Function of Initial pH.

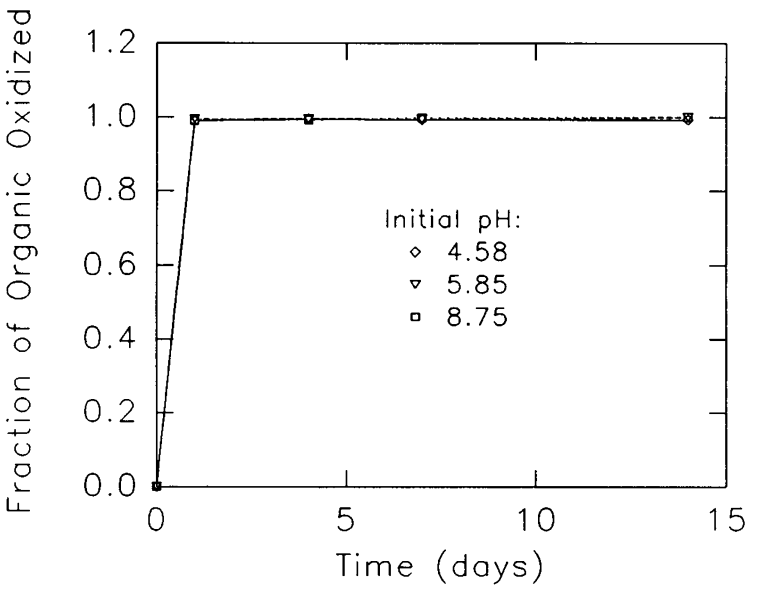

FIGURE 4. Temporally Varying Fraction of Organic Substrate Oxidized During Reductive Dissolution as a Function of pH.

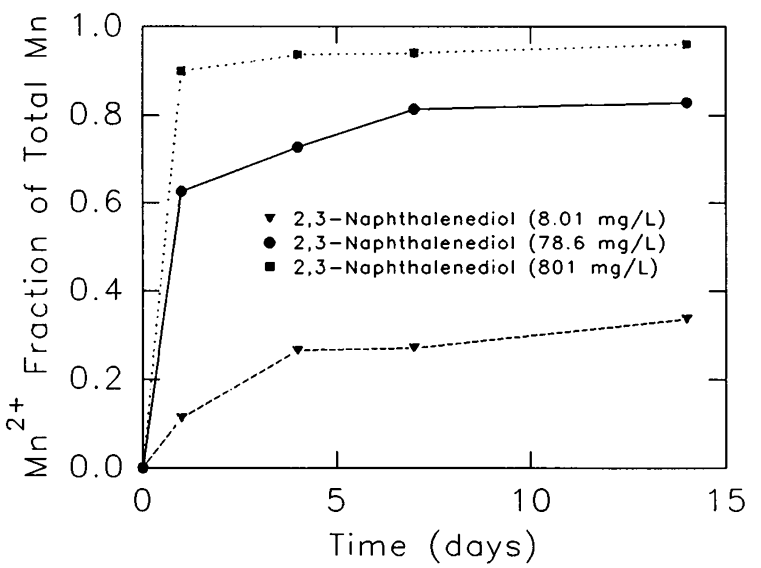

FIGURE 5. Temporally Varying Fraction of Total Manganese as Dissolved Mn^{2+} as a Function of Naphthalenediol Concentration.

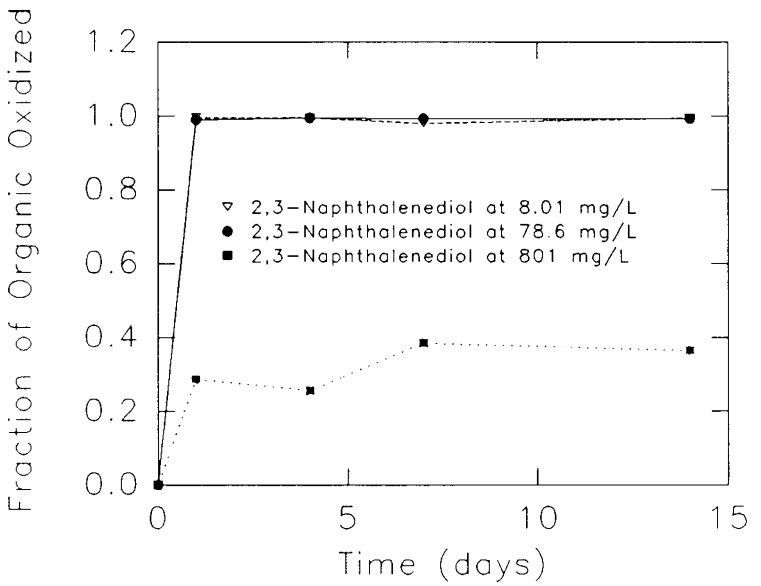

FIGURE 6. Temporally Varying Fraction of Organic Substrate Oxidized During Reductive Dissolution as a Function of Naphthalenediol Concentration.

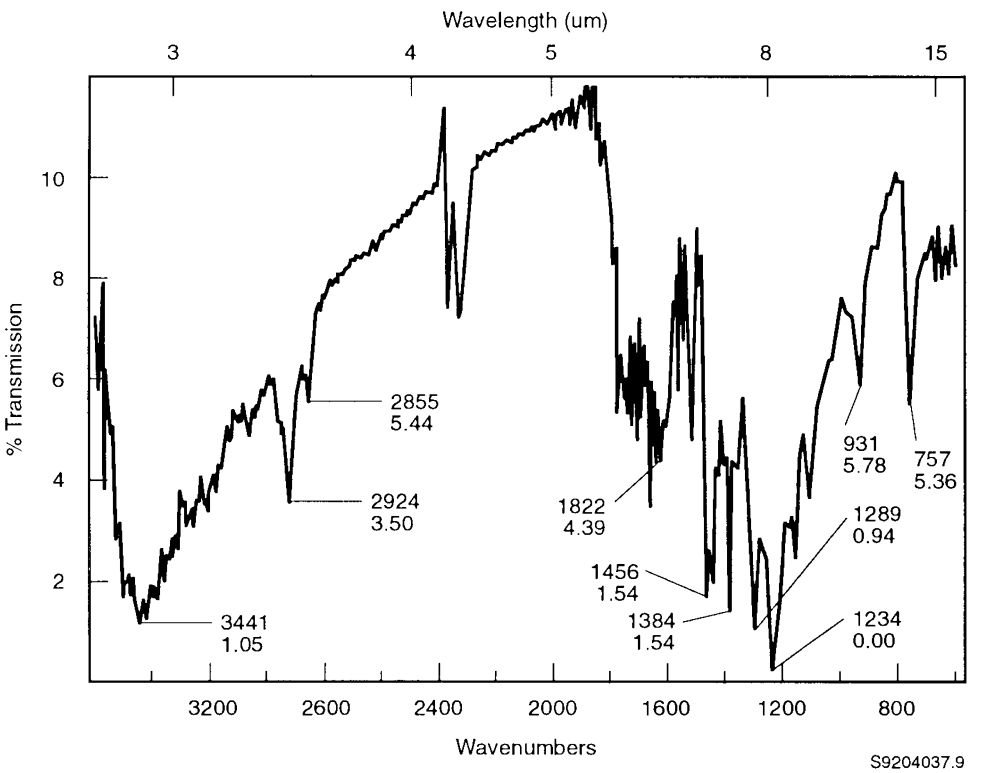

FIGURE 7. Infrared Spectroscopy of Naphthalenediol Residue.

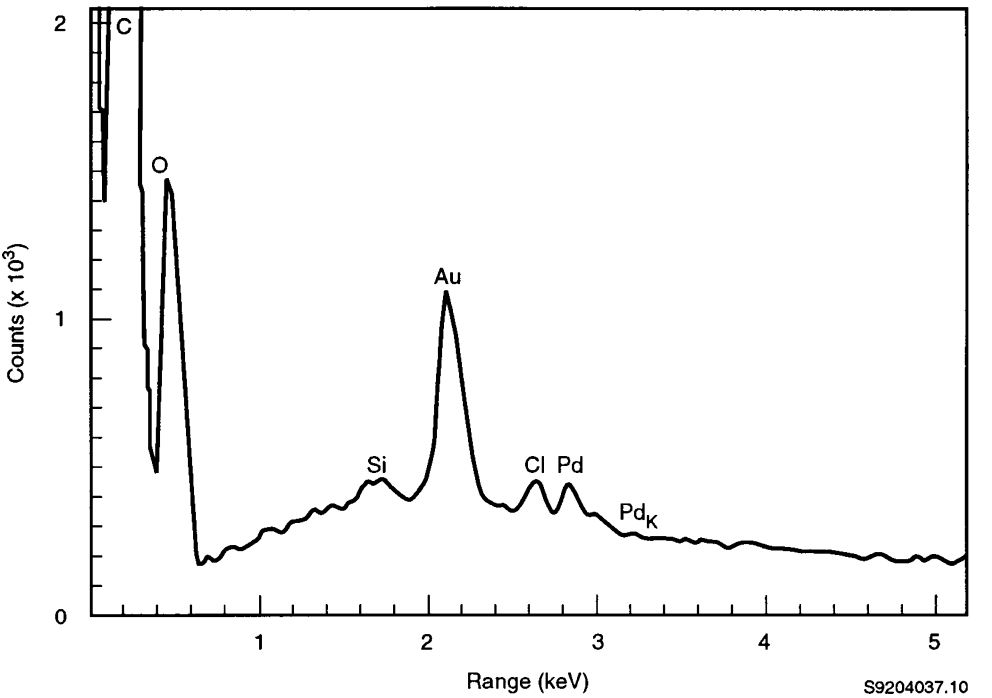

FIGURE 8. Energy-Dispersive X-Ray Analysis of Residue.

DISCUSSION

Characteristics of Manganese Oxide Particles

After 12 months of aging, the specific surface area of the MnO_2 particles, based on identical triplicates, was determined as 179.2 ± 0.5 m^2/g, which when adjusted for time represents a similar area as that reported by Godtfredsen [18] (i.e., 139 versus 137 m^2/g). The high surface area is consistent with the CEC and PZNC results presented in Figure 2. The CEC of the MnO_2 particles, as illustrated in Figure 2, is extremely high and corresponds in magnitude to soil organic matter. Helling et al. [20] published CEC information pertaining to clay and soil organic matter. For a pH range of 2.5 to 8.0, the typical CEC of 60 Wisconsin soils for organic matter and clay ranged from 360 to 2130 $mmol_c/kg$ and from 380 to 640 $mmol_c/kg$, respectively.

Because there is no point where the CEC and AEC curves are equal in magnitude, the PZNC can not be definitively determined from Figure 2. Godtfredsen [18] notes that due to the highly acidic nature of these synthetic MnO_2 particles, surface-charge measurements tend to be problematic. For example, stable, consistent, and reproducible charges are difficult to accurately measure on MnO_2 particles at pH values below 3.1 because MnO_2 is not very stable below this pH [17,18]. The difficulty in determining the PZNC for these oxide particles under low pH conditions is exemplified in Figure 2 and suggests a low PZNC. The high specific surface area, high CEC, small particle size, and low PZNC indicate that the particles have characteristics which lend themselves to being reactive.

Effects of pH on Reductive Dissolution of Manganese Oxide Particles

Following previous research [5,21,22], Whelan and Sims [15] have suggested that the reductive-dissolution/organic-oxidation process could move through a free-radical formation

prior to polymerization. Stone and Morgan [23] have mechanistically described this reductive-dissolution/oxidation process in four steps: 1) precursor-complex formation (i.e., reductant adsorption), 2) electron transfer, 3) release of oxidized organic product, and 4) release of reduced metal ion. They have suggested that the process is surface chemically controlled and not transport controlled. Whelan and Sims [15], therefore, assumed that electron transfer/release of aromatic organic is the rate-limiting step and reduced the four steps outlined above to the following equations, accounting for proton consumption:

$$>Mn^{IV}(OH)_2 + 2\ Nap\text{-}(OH)_2 \underset{k_{-1}}{\overset{k_1}{<\!=\!=\!>}} >Mn^{IV}(O\text{-}Nap\text{-}OH)_2 + 2\ H_2O \quad (1)$$

$$>Mn^{IV}(O\text{-}Nap\text{-}OH)_2 + n\ H^+ \xrightarrow{k_2} Mn^{2+} + H_2O + \text{oxidized products} \quad (2)$$

where k_1 and k_2 are rate constants in the forward direction and k_{-1} is a rate constant in the reverse direction. Assuming that the only species that contribute to the surface mass balance equation are $>Mn^{IV}(OH)_2$ and $>Mn^{IV}(O\text{-}Nap\text{-}OH)_2$ [23,24], and that other competing anions and cations are not considered, the surface mass balance equation is simplified to:

$$S_T = [>Mn^{IV}(OH)_2] + [>Mn^{IV}(O\text{-}Nap\text{-}OH)_2] \quad (3)$$

The total Mn associated with the system (Mn_T) can be expressed as

$$Mn_T = [>Mn^{IV}(OH)_2] + [>Mn^{IV}(O\text{-}Nap\text{-}OH)_2] + Mn^{2+} \quad (4)$$

By combining Equations (1), (2), and (4), and by using a similar approach as that presented by Stone and Morgan [23] and Whelan and Sims [15], the rate of change of Mn^{2+} can be determined as follows:

$$\frac{d[Mn^{2+}]}{dt} = \frac{k_2\,([Mn_T] - [Mn^{2+}])\,\{H^+\}^n\,[Nap\text{-}(OH)_2]^2}{((k_{-1} + k_2\,\{H^+\}^n) / k_1) + [Nap\text{-}(OH)_2]^2} \quad (5)$$

where $\{H^+\}$ represents the proton activity with the total number of remaining sites at time t being $[Mn_T] - [Mn^{2+}]$.

Equations (2) and (5) describe the functional role that protons play in the reductive-dissolution process during the oxidation of aromatics in an oxic environment. Protons are consumed in this process, and a decrease in the pH should increase the reductive-dissolution rate. The results presented in Figure 3 follow the shape suggested by Equation (5) with the Mn^{2+} redox rate increasing with an increasing proton concentration. The significant drop off in Mn^{2+} reduction for the naphthalenediols after the first day corresponds to the 1) near complete oxidation of these organics (Figure 4) and 2) auto-catalytic effect of the Mn oxide in promoting organic oxidation. Figure 3 also demonstrates that as pH increases the rate of reductive dissolution decreases. Mathematically, Equation (5) describes the relationship between the rate of Mn^{2+} production, and pH and naphthalenediol concentrations. If electron transfer/organic release is rate limiting, then $k_1 >> k_2$, and k_{-1} is most likely much larger than "$k_2\,\{H^+\}^n$," thereby reducing Equation (5) to

$$\frac{d[Mn^{2+}]}{dt} = \frac{k_2\,([Mn_T] - [Mn^{2+}])\,\{H^+\}^n\,[Nap\text{-}(OH)_2]^2}{(k_{-1} / k_1) + [Nap\text{-}(OH)_2]^2} \quad (6)$$

If $(k_{-1} / k_1) << [Nap\text{-}(OH)_2]^2$, which may be the case during the initial phases of the experiment when excess organic substrate is present, as illustrated by Stone and Morgan [24], then Equation (6) reduces to

$$d[Mn^{2+}]/dt = k_2 ([Mn_T] - [Mn^{2+}]) \{H^+\}^n \quad (7)$$

Stone and Morgan [24] proposed a similar empirical equation for hydroquinone:

$$d[Mn^{2+}]/dt = k_3 ([Mn_T] - [Mn^{2+}]) \{H^+\}^m [QH_2] \quad (8)$$

where k_3 is a rate constant, m is a constant equaling 0.46, and QH_2 is hydroquinone. During the initial phases of the reductive-dissolution process when the hydroquinone concentration does not change significantly, as illustrated by Stone and Morgan [24], hydroquinone can be considered in excess and a constant, as such Equation (8) can be rewritten as follows:

$$d[Mn^{2+}]/dt = k_4 ([Mn_T] - [Mn^{2+}]) \{H^+\}^m \quad (9)$$

in which

$$k_4 = k_3 [QH_2] \quad (10)$$

where k_4 is a rate constant. When the organic substrate is in excess, Equations (7) and (9) have the same form. A similar type of analysis can be employed when the remaining organic substrate has been nearly completely oxidized {i.e., $(k_{-1} / k_1) >> [Nap\text{-}(OH)_2]^2$}; Equation (6) can be rewritten as follows:

$$d[Mn^{2+}]/dt = k_5 ([Mn_T] - [Mn^{2+}]) \{H^+\}^n [Nap\text{-}(OH)_2]^2 \quad (11)$$

in which

$$k_5 = (k_1 / k_{-1}) k_2 \quad (12)$$

Equation (11) is very similar to Equation (8).

Stone [6] performed a similar analysis using phenol when determining the exponent on the proton concentration by solving the following equation:

$$d[Mn^{2+}]/dt = k_6 \{H^+\}^m [phenol]^p \quad (13)$$

where k_6 is a constant and p is an exponent. He solved for the exponent m and found that it ranged from <0.5 when pH of 4 was approached to greater than unity for pHs greater than 6. Equation (13) is very similar in form to Equation (11).

An analysis can be performed to estimate the exponent "n" on the proton concentration in Equation (11). The condition associated with Equation (11) is chosen {i.e., $(k_{-1} / k_1) >> [Nap\text{-}(OH)_2]^2$}, as opposed to that associated with Equation (7) {i.e., $(k_{-1} / k_1) << [Nap\text{-}(OH)_2]^2$}, because most of the dissolved Mn(II) and naphthalenediol data collected represent long-term information (i.e., on the order of weeks) (see Figures 3 and 5).

Whelan and Sims [15] suggested the following equation, which includes auto-catalysis, for describing the temporal change in Mn reductive dissolution:

$$[Mn^{2+}] = [Mn_T] \{1 - \exp (- \frac{k_7 t}{K_m (K_m + t)})\} \quad (14)$$

where k_7 and K_m are constants, which are related to the rate equations and their corresponding rate coefficients as discussed by Whelan and Sims [15]. The derivations outlined by Whelan and Sims [15] have shown that shape of the curve exhibited by Equation (14) satisfies the conditions for electron transfer/organic release as the rate-limiting step.

By taking the derivative of Equation (14) with respect to time:

$$\frac{d[Mn^{2+}]}{dt} = \frac{k_7 ([Mn_T] - [Mn^{2+}])}{(K_m + t)^2} \quad (15)$$

and combining Equation (15) with Equation (11), the following expression can be derived:

$$\frac{d[Mn^{2+}]}{dt} = \frac{k_7 ([Mn_T] - [Mn^{2+}])}{(K_m + t)^2} = k_5 ([Mn_T] - [Mn^{2+}]) [Nap\text{-}(OH)_2]^2 \{H^+\}^n \quad (16)$$

Linearizing Equation (16) gives

$$Log \{RATIO\} = Log \{k_5 [Nap\text{-}(OH)_2]^2\} - n\ pH \quad (17)$$

in which

$$RATIO = k_7 / (K_m + t)^2 \quad (18)$$

Day 14 results of Equation (17) are plotted in Figure 9 with a coefficient of determination (r^2) of 96%. The negative slope of the curve represents the exponent "n" and has a value of 0.4, which is similar to the value of 0.46 that Stone and Morgan [24] found for the oxidation of hydroquinone using reductive dissolution. Figure 9 represents the interrelationship between pH and the ligand and illustrates the integrated impacts of pH on the oxidation of the ligand [see Equations (17) and (18)], even though it is difficult to visually see the impacts from Figure 4

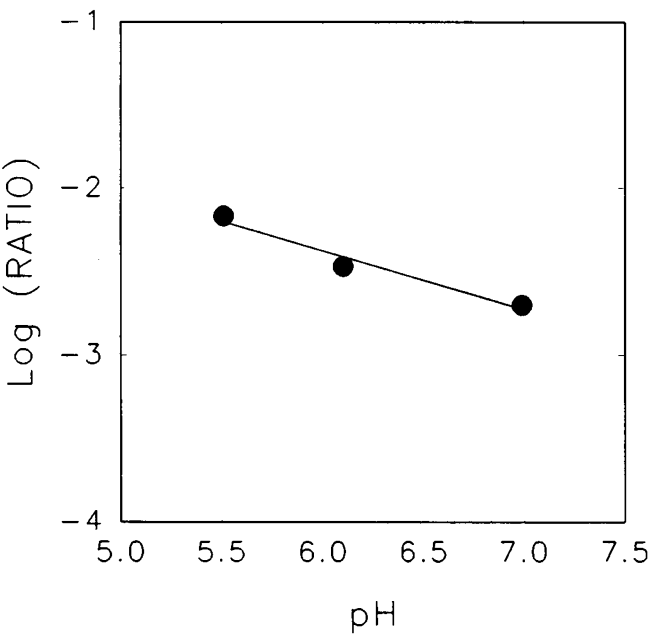

FIGURE 9. Log(RATIO) Versus pH.

alone. According to the mechanisms outlined by Whelan and Sims [15], two organic molecules are required to reduce one manganese (i.e., naphthalenediol is a ½-equivalent reductant). This does not mean that the two ligand sites are simultaneously occupied by two naphthalenediol molecules. The manganese is completely reduced when a second ligand is oxidized at the same active site, thereby making it available for release from the surface. This can be seen by inspecting Figures 5 and 6 (e.g., 801 mg/L). When most of the active sites are occupied (i.e., high organic concentration), most of the oxide surface is reduced and released into solution (i.e., there are plenty of substrate to reduce to manganese at each active site). The impacts of Figure 6 are indicated by Equations (7) and (11) and the assumptions associated with their development.

Effects of Concentration on Reductive Dissolution of Manganese Oxide Particles

The relationship between the rate of reductive dissolution of Mn (i.e., $d[Mn^{2+}]/dt$) and organic-substrate concentration is described by Equation (5). If the 1) initial organic concentrations are very small such that $[Nap\text{-}(OH)_2]^2\} << \{(k_{-1} + k_2 \{H^+\}^n) / k_1\}$, 2) solution is buffered (i.e., constant pH), and 3) amount of dissolved Mn is small relative to the total Mn in the system (i.e., $Mn_T >> Mn^{2+}$), then Equation (5) reduces to the following:

$$\frac{d[Mn^{2+}]}{dt} = \frac{k_2 [Mn_T] \{H^+\}^n [Nap\text{-}(OH)_2]^2}{((k_{-1} + k_2 \{H^+\}^n) / k_1)} \qquad (19)$$

Equation (19) assumes that the rate-limiting step is electron transfer/organic release. Physically, Equation (19) states that the production of reduced Mn(II) is proportional to the square of the organic-substrate concentration when a majority of the reaction sites on the Mn oxide particle are not occupied by the substrate. When the fraction of surface sites occupied by the substrate is high, then the reductive-dissolution rate that is given by Equation (5) will be less than that predicted by Equation (19), asymptotically reaching a constant as illustrated by the shape of a rectangular hyperbola. At this point, a change in the concentration has little influence on the reductive-dissolution rate as all reaction sites are occupied.

Figure 6 presents the fraction of the total Mn as Mn^{2+} as a function of time for three different organic concentrations for 2,3-naphthalenediol: 8.01, 78.6, and 801 mg/L. After the first day, 11% of the total Mn in the 8 mg/L sample was reduced, while 63% and 90% of the total Mn was reduced in the 79 and 801 mg/L samples, respectively. For a "ten-fold" rate of increase in the initial organic-substrate concentration from 8 to 79 mg/L and from 79 to 801 mg/L over the first day, the rate of reductive dissolution only increased by factors of five and two, respectively. This relatively slow increase in the reductive-dissolution rate indicates that many of the oxide sites are occupied well before the first day's sampling, suggesting that a significant portion of the Mn has already been reduced (see Figure 6).

Figure 7 supports these conclusions as it presents the fraction of the organic oxidized (i.e., the molar ratio of the organic oxidized to organic control). By the first sample period (i.e., Day 1), nearly 100% of the parent organic for the 8 and 79 mg/L sampling vessels had been oxidized, while for the 801 mg/L sample, only 29% of the organic had been oxidized. The sharp decrease in the oxidized material in the 801 mg/L sample was due to the near complete reduction in Mn oxide particles [Mn(IV)] to Mn(II) (see Figure 6). The drop off in Mn^{2+} reduction for the naphthalenediols after the first day corresponds to the 1) near complete oxidation of these organics and 2) auto-catalytic effect of the Mn oxide in promoting organic oxidation.

Naphthalenediol Residue from Reductive-Dissolution Process

Whelan and Sims [15] have demonstrated that certain multiple-ringed aromatics in an oxic environment can be significantly oxidized in a metal-oxide reductive-dissolution process, thereby producing insoluble organic matter. Equation (2) suggests that if a free radical represented an

intermediate step, one potential product of abiotic-catalyzed, reductive dissolution was an oxidized or "humified" polymer. The experimental precipitate observed in this study had a deep, dark-brown color, similar to that exhibited by humic polymers. It was insoluble in dichloromethane, acetonitrile, and water at various pHs (3 to 9), and extremely hydroscopic, even though the sample had been dried in a 103 °C oven for 24 hours.

Figure 7 presents the IR results for the precipitate. Various bands occur near 3440, 2924, 2855, 1622, 1456, 1384, 1289, and 1234 cm^{-1}, and at other bands in the fingerprint region (i.e., < 1400 cm^{-1}). Based on previous analyses by Stevenson [25], this spectral curve appears to correspond to an organic compound similar in nature to that of a polymerized naphthalenediol product [16].

The distribution of carbon, oxygen, and hydrogen by weight in naphthalenediol is 75.0%, 20.0%, and 5.0%, respectively. A microelemental analysis determined the composition based on weight of the organic residue as 63.7%, 25.2%, and 4.2% of carbon, oxygen, and hydrogen, respectively, thereby accounting for 93.1% of the total mass; 6.9% is unaccounted for. Illustrative results of the EDXRA are presented in Figure 8 and were used to identify the remaining 6.9% of the mass as that of chloride. Chloride appeared in residue samples but did not appear in background samples. The percentages by weight of the chloride in particle samples ranged from 2.5% to 8.0%. The chloride originates from the $NaClO_4$, which was used to fix the ionic strength of each solution. At a concentration of 10^{-3} M, $NaClO_4$ can supply plenty of available chloride. The 5.2% oxygen in excess of that present in the naphthalenediol (i.e., 20.0% versus 25.2%) could be attributed to the perchlorate ion (ClO_4^-) or oxygen molecules that present in the oxic environment. Lee and Huang [26] note that Mn(III/IV) oxides are able to adsorb and polarize oxygen molecules, leading to the cleavage of the ring structure of polyphenols.

CONCLUSION

A theoretical approach was presented to describe the reductive-dissolution process under various pH and concentration conditions for 2,3-naphthalenediol. The experimental results mirrored those expressed by the derived equations, which suggest that the rate-limiting step is electron transfer/organic release. As the pH decreased or the organic concentration increased, the rate of dissolution increased, confirming an increase in the consumption of protons or utilization of Mn-surface active sites, respectively. The mathematical formulations are also consistent with the results of other researchers [23,24].

Production of by-products of a polymerized residue in an oxic environment helps to support the reductive-dissolution concept of free radicals as the focal point for residue production. Although free radicals were not monitored for, free-radical formation in an oxic environment would be consistent with the theory and results of other researchers [4,27,28]. Because the residue was insoluble in water at pH values ranging from ≈3 to ≈9 and in solvents (i.e., acetonitrile, dichloromethane, and water), the results demonstrate that multiple-ringed aromatics can be oxidized to produce products which may not be readily available as a mobile substance in subsurface systems. Although not specifically addressed herein, the polymerized products may also be less toxic to organisms.

ACKNOWLEDGMENTS

Funding for this research was supplied by the U.S. Geological Survey and U.S. Environmental Protection Agency's Robert S. Kerr Environmental Research Laboratory (through Dynamac Corporation) through grants to Utah State University (USU) under Award Nos. 14-08-0001-G1723 and 68-C8-0058, respectively. Thanks are extended to Drs. J. J. Jurinak, D. K. Stevens, and M. J. Wright of USU, J.-M. Bollag of Pennsylvania State University, A. T. Stone of Johns Hopkins University, and P. M. Huang of the University of Saskatchewan, and Ms. J. McLean of USU for providing valuable technical information during various phases of this work.

Thanks are also extended to Mr. C. Zoch of USU for providing technical assistance with the infrared spectroscopy, Huffman Laboratories of Golden, Colorado, for performing the microelemental analysis, and Mr. W. McManus of USU for performing the energy-dispersive x-ray analysis. Appreciation is extend to Mr. W. R. Gorst of Battelle, Pacific Northwest Laboratories and Ms. L. Hemphill of the Utah Water Research Laboratory for performing the editorial review of this manuscript.

REFERENCES

1. Lindsay, W. L. Chemical Equilibria in Soils, Wiley, New York (1979).

2. Stumm, W. and Morgan, J. J. Aquatic Chemistry, 2nd ed., Wiley, New York, 1981.

3. Ulrich, H.-J. and Stone, A.T. Environ. Sci. Technol, 23, 421 (1989).

4. Fukuzumi, S., Ono, Y. and Keii, T. Int. J. Chem. Kinet, 7, 535 (1975).

5. Shindo, H. and Huang, P. M. Soil Sci. Soc. Amer. J, 48, 927 (1984).

6. Stone, A. T. Environ. Sci. Technol, 21, 979 (1987).

7. Mihelcic, J. R. and Luthy, R. G. Appl. Environ. Microbiol, 54, 1182 (1988).

8. Abbott, C. A. and Sims, R. C. Proceedings of SUPERFUND '89, Hazardous Materials Control Research Institute, Silver Spring, MD, 1989, 23.

9. Keck, J. Investigation of Co-Oxidation of Polynuclear Aromatic Hydrocarbons in Soil Systems, Master's Thesis, Utah State University, Logan, UT, 1989.

10. Bollag, J.-M. and Myers, C. Sci. Tot. Environ, 117, 357 (1992).

11. Bollag, J.-M. and Liu, S.-Y. Pesticides in the Soil Environment, Cheng, H. H., Ed., Soil Science Society of America, Madison, WI, 1990, 169.

12. Cheng, H. H., Haider, K. and Harper, S. S. Soil Biol. Biochem, 15, 311 (1983).

13. Martin, J. P., Haider, K. and Linhares, L. F. Soil Sci. Soc. Am. J, 43, 100 (1979).

14. Whelan, G. and Sims, R. C. Haz. Waste Haz. Mat, 9, 245 (1992).

15. Whelan, G. and Sims, R. C. Mn-Catalyzed Oxidation of Multiple-Ringed Aromatics, Haz. Waste Haz. Mat, (1995) (accepted).

16. Whelan, G. Surface-Induced Oxidation of Multiple-Ringed Diol and Dione Aromatics by Manganese Dioxide, Ph.D. Dissertation, Utah State University, Logan, UT, 1992.

17. Murray, J. W. J. Colloid. Inter. Sci, 46, 357 (1974).

18. Godtfredsen, K. L. Release of MnO_2-Bound Co, Ni, and Cu by Acidification, Competitive Sorption, Complexation, and Reductive Dissolution, Ph.D. Dissertation, The Johns Hopkins University, Baltimore, MD, 1992.

19. Pfaff, J. D., Brockoff, C. A. and O'Dell, J. W. Test Method: The Determination of Inor-

ganic Anions in Water by Ion Chromatography - Method 300.0, U.S. Environmental Protection Agency, Environmental Monitoring and Systems Laboratory, Cincinnati, OH, 1989.

20. Helling, C. S., Chesters, G. and Corey, R. B. Soil Sci. Soc. Am. J, 28, 517 (1964).

21. Senesi, N. and Schnitzer, M. Soil Sci, 123, 224 (1977).

22. Wang, T. S. C., Kao, M.-M. and Huang, P. M. Soil Sci, 129, 333 (1980).

23. Stone, A. T. and Morgan, J. J. Aquatic Surface Chemistry, Stumm, W., Ed., Wiley, New York, 1987, 221.

24. Stone, A. T. and Morgan, J. J. Environ. Sci. Technol, 18, 450 (1984).

25. Stevenson, F. J. Humus Chemistry: Genesis Composition, Reactions, Wiley, New York, 1983.

26. Lee, J. S. K. and Huang, P. M. "Photochemical effect on the abiotic transformations of polyphenolics as catalyzed by Mn(IV) oxide," First Workshop of Working Group MO of the Int. Soc. Soil Sci. on Impact of Interactions of Inorganic, Organic, and Microbiological Soil Components, Edmonton, Canada, 1992.

27. McBride, M. B. Soil Sci. Soc. Am. J, 51, 1466 (1987).

28. Schnitzer, M. Whither Soil Research, Publications of the 12th Int. Congr. Soil Sci., New Delhi, India, 5, 67 (1982).

Address reprint requests to:

Dr. Gene Whelan
Battelle, Pacific Northwest Laboratories
P.O. Box 999
Richland, Washington 99352
509-372-6098 (W) or 509-372-6089 (F)